Simulating bottom-up effects on predator productivity and consequences for the rebuilding timeline of a depleted population

Andre Buchheister [a,b,*], Michael J. Wilberg [b], Thomas J. Miller [b], Robert J. Latour [a]

[a] Virginia Institute of Marine Science, College of William & Mary, P.O. Box 1346, Gloucester Point, VA 23062, USA
[b] Chesapeake Biological Laboratory, University of Maryland Center for Environmental Science, P.O. Box 38, Solomons, MD 20688, USA

ARTICLE INFO

ABSTRACT

Bottom-up control within ecosystems is characterized, in part, by predator populations exhibiting growth and recruitment changes in response to variability in prey density or production. Annual prey availability can vary more than 10-fold in marine ecosystems, with prey experiencing a dramatic increase or pulse in production within some years. To assess the bottom-up effects of such pulses on predator growth, production, and fisheries management, we developed an age-specific, predator–prey simulation model (parameterized for summer flounder, *Paralichthys dentatus*) based on simple hypothesized mechanisms for consumption, growth, and population dynamics. Pulses in each of the three modeled prey groups (small crustaceans, forage fish, larger fish prey) generated different magnitudes of change in predator weight-at-age (w), spawning stock biomass (S), fishery yield (Y), and recruitment (R), due to ontogenetic differences in growth potential and dietary composition across predator age classes. Increases in productivity of small forage fishes generated the greatest gains in predator w, S, Y, and R, relative to pulses of the other prey groups. Median increases in R following a prey pulse were minimal (<4%) except under high fishing rates that stimulated a stronger compensatory response in the population (8–11% increase in R), demonstrating the interactive role of top-down and bottom-up effects on predator productivity. Seasonal migration patterns determined the degree of spatiotemporal overlap of predators with the spatially constrained pulses in prey production. Prey pulses reduced the median time required for depleted populations to be rebuilt by 0–5% following declines in fishing pressure. Reductions in time to recovery were highly variable due to recruitment stochasticity, but stock recovery was more sensitive to the severity of harvest control measures than to availability of the non-limiting prey. Understanding the relative magnitudes of such bottom-up processes, particularly in the presence of varied fishing pressure can aid in developing ecosystem approaches to fisheries management that account for such ecological interactions more explicitly.

© 2015 Elsevier B.V. All rights reserved.

1. Introduction

Bottom-up control in ecosystems is characterized by the regulation of higher-trophic-level productivity and variability by processes acting on lower trophic levels. Although other forms of control (top-down and wasp-waist) can be dominant in some systems or under certain conditions (Hunt and Stabeno, 2002; Cury and Shannon, 2004; Hunt and McKinnell, 2006), empirical evidence supports bottom-up structuring of various marine ecosystems (Aebischer et al., 1990; Verheye, 2000; Chavez et al., 2003; Frederiksen et al., 2006). Theoretically, a simple mechanism supporting such bottom-up control can consist of four steps: (1) environmentally mediated increases in prey production and density, (2) enhanced foraging by predators, (3) improved growth, survival, and fecundity of predators, and (4) greater recruitment to the following generation of the predator population. The relationship between predator density and prey density that would link the two ends of this mechanistic progression has been described in terrestrial literature as a predator's reproductive numerical response (Solomon, 1949; Holling, 1959). For marine fishes, direct empirical support for such a mechanism is stronger for steps 1–3 (e.g., McGowan et al., 1998; Ringuette et al., 2002; Castonguay et al., 2008), but wanes through its progression to step 4 (e.g., Mcfarlane and Beamish, 1992; Beaugrand et al., 2003). Thus, at broad scales, support for reproductive numerical responses by fishes tends to be more correlative in nature (Aebischer et al., 1990; Ware and Thomson, 2005; Frank et al., 2007), with the mechanistic components corroborated empirically at smaller spatiotemporal scales or supported theoretically.

* Corresponding author at: Chesapeake Biological Laboratory, University of Maryland Center for Environmental Science, P.O. Box 38, Solomons, MD 20688, USA. Tel.: +1 410 326 7396; fax: +1 410 326 7264.
E-mail address: andrebuc@umces.edu (A. Buchheister).

Two of the main difficulties in linking prey and predator densities at system-wide scales involve the high degree of interannual variability in predator–prey populations and the adaptive foraging behaviors of most fishes. Populations of fishes and other organisms commonly experience 10-fold variability in recruitment, but variations can be even more drastic (>100-fold) as recruitment and mortality are influenced by a complex suite of climatic, oceanographic, ecological, and anthropogenic factors (Rothschild, 1998; Hunt and Stabeno, 2002; Houde, 2009). Importantly, an aggregation of ameliorative conditions in some years can cause dramatic increases, or pulses, in production (Holland et al., 1987; Rothschild, 1998; Jung and Houde, 2004b). These pulses in production can be targeted and consumed heavily by predators, especially by relatively opportunistic fishes that can switch to these prey as they become more available (Ringuette et al., 2002; Castonguay et al., 2008). However, the ability of predators to exploit pulses in prey production is partially mediated by ontogenetic changes in diets and food preferences (Scharf et al., 2000). Years of abrupt failures in prey production or recruitment can also have important consequences for predator populations (Gjøsæter et al., 2009). Understanding a predator's growth and numerical responses to the large inherent variability in prey production can be an important component to characterizing the trophodynamic mechanisms controlling fisheries production.

The potential benefits of increased prey production to predators can interact with top-down fishing pressure and be influenced by spatiotemporal overlap of the interacting species. For exploited predator populations, fishery removals are a dominant source of mortality, and a reproductive numerical response could be dissipated by the harvest of any surplus predator production that results from prey pulses. Movement of predatory populations also has the potential of obscuring any bottom-up effects, given that prey production can be regionally confined. For example, many marine fishes have life histories dependent on estuaries, in which prey production can be greater relative to alternative offshore habitats (Beck et al., 2001; Able, 2005). Thus, the degree of movement between estuarine and offshore regions could influence predator–prey overlap, predatory growth, and the numerical response.

In this study, we evaluated the population-scale consequences of increased prey availability on a predator stock using a mechanistic, multi-species simulation model, parameterized for summer flounder, *Paralichthys dentatus*. The age-specific, spatial, predator–prey model linked consumption, growth, and population dynamics. Summer flounder was chosen as the model predator because its fishery and ecology (e.g., migration, ontogenetic diet shifts, life history) are representative of other exploited marine groundfish, and because there is evidence that the species is responsive to pulses in prey production. This species has supported a large fishery in the northwest Atlantic Ocean, and overfishing led to significant declines of the stock, reaching record lows in the late 1980s (Terceiro, 2002). After establishing a rebuilding plan and implementing regulations, the stock recovered and was declared rebuilt in 2010 (Terceiro, 2011). Based on research from the Chesapeake Bay (the largest estuarine nursery area serving the coastal summer flounder population), summer flounder demonstrated strong episodic increases in prey consumption likely driven by prey availability (Buchheister and Latour, 2015b). These annual periods of increased consumption were also correlated with larger weight-at-age for summer flounder (Buchheister, unpublished data).

Our simulation model provided a controlled virtual environment for examining questions regarding the potential population-scale response to pulses in prey production. We were specifically interested in examining the relative effects of three different prey groups that are consumed and targeted at varying rates through ontogeny, as is common in the diets of many fishes (Latour et al., 2008; Buchheister and Latour, 2015a). Multiple modeling scenarios were used to address three major research questions: (1) How do pulses in productivity of different prey populations influence the growth, production, and reproductive numerical response of a migratory predator? (2) How do fishing rates and migration patterns interact with a population's ability to harness regionally localized increases in prey production? (3) What influence would these prey pulses have on rebuilding timelines of an overfished predator population? Understanding the relative magnitudes of these bottom-up processes, particularly in the presence of varied fishing pressure can aid in developing ecosystem approaches to fisheries management that account for such ecological interactions more explicitly (Link, 2010a).

2. Methods

2.1. Base model formulation

We developed a spatial, age-specific simulation model that consisted of linked population, growth, and consumption models. Within the population model, the key abundance changes modeled were decreases in abundance due to fishing and natural mortality, movement between regions, and additions through recruitment (Fig. 1). The model was parameterized to represent the summer flounder stock along the Northeast U.S. Atlantic coast, from North Carolina to Maine. We coded the model for two linked spatial domains or ecosystems (region 1 – nearshore estuaries and bays; region 2 – offshore continental shelf waters) to account for the strong migration of the species between these habitats. Summer flounder were modeled with 8 age-classes from age-0 to age-7+, following the convention of recent stock assessments (Terceiro, 2011). We treated time discretely, using a seasonal (3-month) time-step to account for the highly seasonal dynamics of summer flounder movement, spawning, and growth. Within each time step, the order of processes proceeded with recruitment, mortality, consumption, growth, and movement, with the census taken at the end of each season. Model simulations were conducted for 55 years under various scenarios (see Section 2.2) following a 25-year burn-in period. All symbols for the simulation model are defined in Table 1. Model equations are presented in Table 2 and referenced by T$x.y$, with x denoting the table number and y indicating the
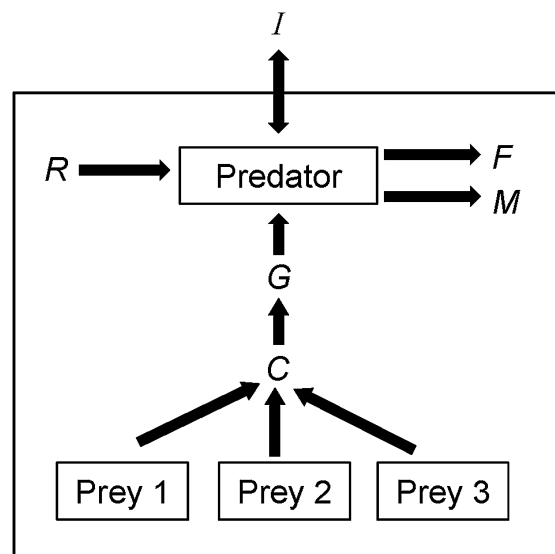

Fig. 1. Diagram of predator–prey simulation model. Major mechanistic processes are labeled (C – consumption, G – growth, R – recruitment, I – net immigration, F – fishing mortality losses, M – natural mortality losses).

Table 1
Description of symbols in Table 2 that were used for the simulation model.

Symbol	Description	Units
Subscript indicators (range/level)		
a	Predator age (0–7+)	Years
A	Maximum predator age; plus group (7+)	Years
j	Prey type (crustaceans = 1, small fishes = 2, larger fishes = 3)	
r	Region (nearshore estuaries and bays = 1, offshore shelf = 2)	
n	Neighboring region (nearshore estuaries and bays = 1, offshore shelf = 2)	
s	Season (Jan–Mar, winter = 1; Apr–Jun, spring = 2; Jul–Sep, summer = 3; Oct–Dec, fall = 4)	
s'	Spawning season (fall)	
y	Year (1–80)	
y^*	Year in which a pulse occurs (5 random years selected from $y = 26$–50)	
Calculated values		
$P_{y,a,s,r}$	Predator abundance by year, age, season, and region	Fish
$I_{y,a,s,r}$	Net immigration by year, age, season, and region	Fish
$R_{y,r}$	Abundance of surviving recruits by year and region in season 1	Fish
$S_{s'}$	Predator spawning biomass in the spawning season	kg
$L_{y,a,s}$	Fraction of fish that survive by year, age, and season	
$F_{y,a,s}$	Instantaneous fishing mortality rate by year, age, and season	Year^{-1}
$G_{y,a,s,r}$	Somatic growth by year, age, season, and region	kg
$w_{y,a,s,r}$	Average individual weight-at-age by year, season, and region	kg
$K_{y,a,s,r}$	Gross conversion efficiency by year, age, season, and region	
$C_{j,y,a,s,r}$	Per capita consumption by prey, year, age, season, and region	kg prey (kg pred)$^{-1}$ s^{-1}
$C_{a,s}^{max}$	Maximum per capita consumption by age and season	kg prey (kg pred)$^{-1}$ s^{-1}
$\bar{w}_{a,s}$	Mean empirical weight-at-age by season	kg
$\alpha_{j,a,s}$	Functional response attack rate coefficient by prey, age, and season	(kg prey)$^{-1}$
$N_{j,y,s,r}$	Prey j biomass year, season, and region	kg
$f_{s,r}$	Proportion of max consumption attainable by season and region	
V, X, Y, Z	Intermediate calculations for f	
Y_y	Biomass yield to the fishery by year	kg
Parameters		
$\phi_{s,n\to r}$	Proportion of predators migrating from region n into region r by age and season	
$\phi_{s,r\to n}$	Proportion of predators migrating from region r into region n by age and season	
F_y	Instantaneous fishing mortality rate by year	Year^{-1}
sel_a	Selectivity of fishery by age	
M	Instantaneous natural mortality rate	Year^{-1}
α_{SR}	Maximum recruitment-per-unit biomass for stock–recruitment relationship	10^6 recruits (kmt)$^{-1}$
κ_{SR}	Threshold biomass above which the density-dependent effects dominate the density-independent effects	kmt
β_{SR}	Shape parameter for degree of density compensation ($\beta = 1$ for Beverton Holt)	
θ_r	Fraction of total recruitment that recruits to region r	
δ_y	Stochastic recruitment error term $\sim N(0, \sigma_\delta^2)$ by year	
$m_{a,s'}$	Proportion of fish that are mature by age during the spawning season	
w_0	Average individual weight of age-0 predator in first season	kg
KL	Maximum gross conversion efficiency	
KR	Rate parameter for change in gross conversion efficiency	g^{-1}
KW	Weight at which K is 50% of KL	g
h	Shape parameter for functional response (Type II when $h = 1$)	
λ_j	Scale parameter for maximum attack rate by prey	(kg prey)$^{-1}$
ρ_j	Rate parameter for change in attack rate with age for prey j	Years^{-1}
η_j	Age at which attack rate is 50% of λ_j	Years
η_{1j}, η_{2j}	Inflection points for ascending and descending limbs of double logistic equation	Years
CA	Intercept for the allometric relationship between C and predator mass	
CB	Rate parameter for the allometric relationship between C and predator mass	
$\bar{N}$	Mean biomass for prey 2	kg
τ_j	Biomass of prey j relative to biomass of prey 2	
$\psi_{y,r}$	Prey biomass multiplier by year and region	
$\gamma_{j,y,s,r}$	Stochastic error term $\sim N(0, \sigma_\gamma^2)$ for prey j biomass by year, season, and region	
$T_{s,r}$	Mean bottom water temperature by season and region	°C
CTM	Maximum water temperature above which consumption ceases	°C
CTO	Optimal water temperature for maximum consumption	°C
CQ	Rate parameter for temperature function	

equation number within the table. All model parameters are presented in Appendix Table A1.

2.1.1. Population dynamics

We modeled the summer flounder population abundance following initial recruitment. Recruitment (i.e., with $a = 0$ and $s = 1$) followed Beverton–Holt stock recruitment (*SR*) dynamics (Eq. (T2.1)) and was dependent on: *SR* parameters presented by Rothschild et al. (2012); the coast-wide annual spawning stock biomass during the spawning season (Eq. (T2.8)); the fraction of the total recruitment that occurs in each region; a stochastic error

term to generate lognormal deviates; and a survivorship equation (Eq. (T2.9)). Given the importance of estuaries as nursery areas for summer flounder, we assumed that 90% of the recruitment occurred in region 1 (Packer et al., 1999). Survivorship was dictated by population declines generated with a constant, instantaneous natural rate ($M = 0.25$) and age-specific annual fishing mortality rates based on age-dependent selectivities (Eq. (T2.10)) following the stock assessment (Terceiro, 2011); due to fishing pressure throughout the year and a lack of adequate information, mortality rates were assumed to be constant across seasons and regions. Following initial recruitment, population abundances for each age and

Table 2
Equations for the summer flounder (*Paralichthys dentatus*) simulation model consisting of population dynamics, growth, and consumption.

Equation	
Population submodel	
Population dynamics (s = 1)	
$P_{y,a=0,s=1,r} = R_{y,r} = \dfrac{\alpha_{SR} S_{y,s'}}{(1 + S_{y,s'}/\kappa_{SR})^{\beta_{SR}}} \theta_r e^{\delta y} L_{y,a,s}$	(T2.1)
$P_{y,a,s=1,r} = (P_{y-1,a-1,4,r} + I_{y,a,s,r}) L_{y,a,s}$	(T2.2)
$P_{y,A,s=1,r} = (P_{y-1,A-1,4,r} + P_{y-1,A,4,r} + I_{y,A,1,r}) L_{y,a,s}$	(T2.3)
$I_{y,a,s=1,r} = \varphi_{s,n \to r} P_{y-1,a-1,4,n} - \varphi_{s,r \to n} P_{y-1,a-1,4,r}$	(T2.4)
$I_{y,A,s=1,r} = \varphi_{s,n \to r}(P_{y-1,A-1,4,n} + P_{y-1,A,4,n}) - \varphi_{s,r \to n}(P_{y-1,A-1,4,r} + P_{y-1,A,4,r})$	(T2.5)
Population dynamics (s > 1)	
$P_{y,a,s,r} = (P_{y,a,s-1,r} + I_{y,a,s,r}) L_{y,a,s}$	(T2.6)
$I_{y,a,s,r} = \varphi_{s,n \to r} P_{y,a,s-1,n} - \varphi_{s,r \to n} P_{y,a,s-1,r}$	(T2.7)
Supporting equations	
$S_{y,s'} = \sum\limits_{r=1}^{2} \sum\limits_{a=0}^{A} P_{y,a,s',r} w_{y,a,s',r} m_{a,s'}$	(T2.8)
$L_{y,a,s} = e^{-0.25(M + F_{y,a})}$	(T2.9)
$F_{y,a} = F_y \cdot sel_a$	(T2.10)
$Y_y = \sum\limits_{s=1}^{4} \sum\limits_{r=1}^{2} \sum\limits_{a=0}^{A} \dfrac{F_{y,a}}{M + F_{y,a}} (1 - L_{y,a,s}) P_{y,a,s,r} w_{y,a,s,r}$	(T2.11)
Growth submodel	
Growth	
$w_{y,a,s,r} = \dfrac{1}{P_{y,s,r,a}}(P_{y,a,s-1,r} L_{y,a}(1 - \varphi_{s,r \to n})(w_{y,a,s-1,r} + G_{y,a,s,r}) + P_{y,a,s-1,n} L_{y,a} \varphi_{s,n \to r}(w_{y,a,s-1,n} + G_{y,a,s,n}))$	(T2.12)
$G_{y,a,s,r} = f_{s,r} K_{y,a,s,r} \sum\limits_{j=1}^{k} C_{j,y,a,s,r}$	(T2.13)
$w_{a=0,s=1,r} = w_0$	(T2.14)
$K_{y,a,s,r} = \dfrac{KL}{1 + e^{-KR(1000 w_{y,a,s,r} - KW)}}$	(T2.15)
Temperature dependence	
$f_{s,r} = V^X e^{(X(1-V))}$	(T2.16)
$V = (CTM - T_{s,r})/(CTM - CTO)$	(T2.17)
$X = \dfrac{Z^2 \left(1 + \sqrt{(1 + 40/Y)}\right)^2}{400}$	(T2.18)
$Y = \ln(CQ) \cdot (CTM - CTO + 2)$	(T2.19)
$Z = \ln(CQ) \cdot (CTM - CTO)$	(T2.20)
Consumption submodel	
Functional response	
$C_{j,y,a,s,r} = \dfrac{C_{a,s}^{max} \alpha_{j,a,s} N_{j,y,s,r}^h}{C_{a,s}^{max} + \sum_{j=1}^{k} \alpha_{j,a,s} N_{j,y,s,r}^h}$	(T2.21)
$C_{a,s}^{max} = 91 \cdot \bar{w}_{a,s-1} \cdot CA(\bar{w}_{a,s-1})^{CB}$	(T2.22)
$\alpha_{j,a,s} = \dfrac{\lambda_j}{(1 + e^{-\rho_j(a_s - \eta_j)})}$	(T2.23)
$\alpha_{j=2,a,s} = \lambda_j \left(\dfrac{1}{(1 + e^{-\rho_j(a_s - \eta_{1j})})}\right) \left(1 - \dfrac{1}{(1 + e^{-\rho_j(a_s - \eta_{2j})})}\right)$	(T2.24)
Prey biomass	
$N_{j,y,s,r} = \bar{N}_2 \tau_j \psi_{y,r} e^{\gamma_{j,y,s,r}}$	(T2.25)

time step were calculated by tracking survivors and accounting for the net movement of fish between regions (Eqs. (T2.2, T2.3, T2.6)). Net movement (*I*) of fish was calculated based on proportions of individuals that migrate from each region to the neighboring region in each season (Eqs. (T2.4, T2.5, T2.7); see also Section 2.2.3). For the plus group, age-*A* predator abundance during s = 1 ($P_{y,A,s=1,r}$) was calculated using the abundances of the surviving members of age-*A* fish plus age-*A*-1 individuals that joined the group (Eq. (T2.3)). To initiate the model, abundances by age in the first year were set to the stock assessment estimates for 1989 (Terceiro, 2011), divided evenly between regions and constant across seasons.

2.1.2. Growth

We used a gross conversion efficiency approach to model the changes in mean weight-at-age of summer flounder through time and space. Any changes in mean individual weight altered the spawning stock biomass of the population and subsequently recruitment. Prior to accounting for mixing between regions, weight-at-age ($w_{y,a,s,r}$) was defined as:

$$w_{y,a,s,r} = w_{y,a,s-1,r} + f_{s,r} K_{y,a,s,r} \sum_{j=1}^{k} C_{j,y,a,s,r} \tag{1}$$

The gross conversion efficiency ($K_{y,a,s,r}$), which is the proportion of prey mass that is converted to somatic mass, was modeled as a decreasing logistic function of weight to account for the physiological decline in growth rate and greater energy allocation to reproduction that occurs through ontogeny ((T2.15); Brett, 1979). The consumption of each prey ($C_{j,y,a,s,r}$) was modeled with a Type-II functional response (see Section 2.1.3). A temperature-dependent function ($f_{s,r}$) scaled the consumption of fish to account for the physiological changes in maximum consumption and growth attainable in different seasons ((T2.16); Hanson et al., 1997). Parameters for $f_{s,r}$ (*CTM, CTO, CQ*; (T2.16–T2.20)) for summer flounder (a temperate species) were modified from a bioenergetics model of a subtropical

congener, *Paralichthys lethostigma* (Burke and Rice, 2002). Seasonal mean temperatures for each region were obtained from monitoring data from the Chesapeake Bay Program and the Northeast Fisheries Science Center (Table A1). We set the initial weight of an age-0 individual in the first season (i.e., 3-month old) as a constant (w_0) derived from empirical data from the Chesapeake Bay (Table A1). The parameterization of the gross conversion efficiency is described below (see Section 2.1.4). To account for mixing of fish from the two regions following their movement, the final seasonal weight-at-age within a region was calculated as an abundance-weighted mean of the individuals that ended in that location (as detailed in Eq. (T2.12)), but for simplicity, Eq. (1) describes the growth process prior to population mixing.

2.1.3. Consumption

We modeled three functional prey groups to represent the majority of general prey types consumed by summer flounder in the wild (Link et al., 2002; Staudinger, 2006; Latour et al., 2008; Buchheister and Latour, 2011). Prey 1 represented small crustaceans such as mysids (e.g., *Neomysis americana*) and shrimps (e.g., *Crangon septemspinosa*), prey 2 represented small forage fishes (e.g., *Anchoa mitchilli*), and prey 3 represented larger fishes (e.g., *Leiostomus xanthurus*) and squid (e.g., *Doryteuthis pealeii*, *Illex illecebrosus*). Biomass of each prey ($N_{j,y,s,r}$) varied stochastically around a mean value based on random lognormal deviates ($e^{\gamma_{j,y,s,r}}$) that were year-, season-, and region-specific (Eq. (T2.25)). The mean biomass for prey 2 ($\bar{N}_2$) was set at 30 kmt (Jung and Houde, 2004a), and biomasses for prey 1 and prey 3 biomasses were scaled (using parameter τ_j) to be an order of magnitude higher and lower than $\bar{N}_2$, respectively, based on their different trophic levels (Link, 2010b). A biomass multiplier (ψ) was used to simulate prey pulses (see Section 2.2.1 for description).

Biomasses of prey species were forced in the model without predator feedbacks under the assumption that top down control of prey by the single modeled predator was negligible. This was done for several reasons. First, each general prey group is representative of multiple, generally shorter-lived species, and they are consumed by a diversity of predators in natural systems such that the influence of a single predator species on the dynamics of the general prey groups would be minimal. For example, based on an ecosystem model of Chesapeake Bay (Christensen et al., 2009), summer flounder (with a trophic level of 3.6) comprise only 1% of the biomass within trophic levels 3.25–3.75, and they account for <5% of the predation mortality on prey that are representative of prey groups 1 and 2 in our model. Second, many temperate marine ecosystems, like the one in which summer flounder reside, are characterized by generalist feeding patterns and weak interactions that hinder strong top-down control of prey populations (Closs et al., 1999; Link, 2002; Frank et al., 2007). Third, we were interested in testing the effects of simulated prey pulses that represent short periods of excessive prey production (see Section 2.2.1 for description of prey pulses). These prey pulses are controlled by density-independent environmental factors, and they can easily overwhelm any top-down control by predators (e.g., Holland et al., 1987; Rothschild, 1998; Jung and Houde, 2004b).

We modeled average, per capita consumption using a type-II multispecies functional response model (Eq. (T2.21); Koen-Alonso, 2007). The functional response model was dependent on prey biomasses, a shape parameter (h), maximum per capita consumption ($C_{a,s}^{max}$), and prey-specific attack rates ($\alpha_{j,a,s}$). We assumed $h = 1$, which corresponds with a hyperbolic type-II functional response (Koen-Alonso, 2007). We estimated $C_{a,s}^{max}$ as an allometric function of mean body weight (Eq. (T2.22)) using values for striped bass (Hartman and Brandt, 1995a) that reproduced size-based empirical trends in maximum stomach fullness of wild summer flounder (Buchheister, unpublished data). To account for observed

ontogenetic transitions in dietary contributions of the three prey (Buchheister and Latour, 2015a, 2015b), we modeled attack rates with an age-dependent logistic decline for prey 1 (Eq. (T2.23)), a dome-shaped double logistic curve for prey 2 (Eq. (T2.24)), and a logistic increase for prey 3 (Eq. (T2.23)). The age-dependent, inflection-point parameters (η) for these attack rate functions were assumed based on trends in empirical diet data (Table A1; Buchheister and Latour, 2015a). Below, we describe and support the parameterization of the functional response model.

2.1.4. Base model calibration

Parameterization of the base model was informed by fishery independent survey data, stock assessment reports, and available literature (Table A1). Few suitable empirical values existed for parameterizing the growth and consumption equations, so we chose parameter values to closely match two empirical relationships: (1) mean weight-at-age of summer flounder based on 4849 individuals captured over 10 years in a fishery-independent trawl survey from Chesapeake Bay (Fig. 2C; Bonzek et al., 2011); and (2) diet composition by age as informed by empirical stomach content data, reflecting ontogenetic transitions in preferred prey (Fig. 2A; Buchheister and Latour, 2015b). We used a two-stage approach to select suitable growth and functional response parameters. First, we estimated the gross conversion efficiency parameters (KL, KR, KW) that regulated growth by minimizing the mean square error of weight-at-age estimates (relative to the empirical model; Fig. 2C). This was done while holding consumption constant at 40% of C^{max}, which is a reasonable level for consumption in the wild (Hartman and Brandt, 1995b; Stevens et al., 2006). Second, we estimated the functional response parameters, λ and ρ (Eqs. (T2.23 and T2.24)), that regulated the prey-specific attack rates and the relative amounts of prey consumption. These parameters helped dictate predatory growth (by affecting the total amount of food consumed) as well as dietary composition. In the absence of empirical data on attack rates and prey biomasses, we calibrated λ and ρ (for all prey simultaneously) to best approximate both the mean weight-at-age and diet composition relationships by minimizing the sum of the mean square errors to those two relationships. This estimation was done while holding prey biomasses constant at their mean values (i.e., without stochasticity). In other words, the parameters dictating the attack rates for each prey were chosen to best approximate the growth and dietary data, but are conditional on the assumed prey biomass and the other parameters in the model.

2.2. Model scenarios

2.2.1. Prey scenarios

With the simulation model, we explored a three-way factorial combination of scenarios involving different prey pulses, fishing pressure, and movement conditions (Table 3). The three prey scenarios involved introducing random pulses in prey production that elevated the standing stock biomass of each prey group above its long-term mean value (Eq. (T2.25)). To induce pulses in prey production, prey biomass was modified using a year- and region-specific biomass multiplier, ψ. For the base model, this parameter was forced to be constant ($\psi = 1$). For each prey scenario, five years ($n_{pulse} = 5$) were randomly selected within a 25-year "experimental" period (defined as years 26–50, following a 25-yr burn in period) during which ψ was assigned a random number between two and six for the nearshore region ($r = 1$) only. This range for ψ was chosen because, on average, it generated a maximum increase of 10-fold for prey biomass levels across simulations (after accounting for the random stochastic variability, which alone generated 2–3-fold differences in N); a 10-fold variability in prey biomass and recruitment is not uncommon (Houde, 2009). The frequency of pulses was based on empirical diet data for summer flounder and other species that

Table 3
Description of simulation scenario levels for prey pulses, fishing mortality, and movement.

Scenarios	Description
Pulse scenario	
Prey 1	5 annual increases in biomass (2–6-fold) of prey group 1, representing small crustaceans (e.g. mysids, shrimps)
Prey 2	5 annual increases in biomass (2–6-fold) of prey group 2, representing small forage fishes (e.g. anchovies)
Prey 3	5 annual increases in biomass (2–6-fold) of prey group 3, representing larger fishes and cephalopods (e.g. sciaenids, squids)
Fishing sub-scenarios	
H	Constant, high fishing mortality (F_{max})
L	Constant, low fishing mortality for maximum sustainable yield (F_{MSY})
D	Linear decrease in fishing mortality from F_{max} to F_{MSY} over 12 years
D2[a]	Linear decrease in fishing mortality from F_{max} to F_{MSY} over 6 years
M[a]	Immediate, knife-edge decrease in fishing mortality from F_{max} to zero
Movement sub-scenarios	
Mig	Seasonal migrations between offshore and nearshore habitats
Mix	Spatially mixed population with equal distribution and movement between offshore and nearshore habitats

[a] These fishing sub-scenarios only used as contrasts to the D sub-scenario for estimating time to recovery.

was indicative of annual pulses in consumption approximately 1–3 times in a 10-year period (Buchheister and Latour, 2015b). In summary, each prey oscillated randomly around its respective mean, but for a given prey scenario, that prey would experience a 2–6-fold increase in biomass (in addition to the stochastic variability) within the nearshore region during 5 random years (Fig. 3).

2.2.2. Fishing sub-scenarios

We developed three sub-scenarios that examined the influence of fishing pressure on the population's response to the simulated prey pulses (Table 3). These three sub-scenarios represented different stages of annual fishing mortality rates experienced by the northwest Atlantic summer flounder population. For sub-scenario H, fishing mortality (F) was held constant and high ($F_{max} = 1.5$), representing the average F in the fishery from 1982 to 1996 (Terceiro, 2011). For sub-scenario L, F was held constant and low ($F_{MSY} = 0.31$), representing the sustainable level of F achieved after successful management and regulation of the fishery. And for sub-scenario D, F declined linearly through time from F_{max} to F_{MSY} over a period of 12 years (starting at year 26 of the simulation), representing the approximate trajectory of F values observed in the summer flounder fishery while fishing pressure was being reduced (Terceiro, 2011). For our simulations, the target F value was set at $F_{MSY} = 0.31$, the fishing mortality that achieved maximum sustainable yield (MSY) in the base model under deterministic conditions (Fig. A1). Spawning stock biomass for MSY (S_{MSY}) was defined as the equilibrium S when F_{MSY} was maintained. Two additional fishing sub-scenarios were generated for comparison with sub-scenario D, but only for assessing the time required to rebuild depleted stocks. For sub-scenario D2, F was reduced twice as fast as sub-scenario D (i.e., a linear decline from F_{max} to F_{MSY} over 6 years), and for sub-scenario M, F mimicked a moratorium (i.e., an immediate shift from F_{max} to $F = 0$ at year 26 of the simulation).

2.2.3. Movement sub-scenarios

To evaluate the role of spatial connectivity in transferring the bottom-up pulses in prey production to the predator population, two movement sub-scenarios were constructed (Table 3). The migration sub-scenario relied on season-specific proportional movements of fish between the two regions. These proportions were assumed based on catch data that describes the summer flounder life history strategy of moving nearshore during summer and offshore for winter (Table A1; Packer et al., 1999; Terceiro, 2002). While there is a small amount of overwintering of age-0 fish in the nearshore area, the majority of the population exhibits a similar migration between the two broadly defined regions (Packer et al., 1999), so we treated movements as constant across ages. This seasonal movement pattern was contrasted with a fully mixed

sub-scenario in which recruitment to regions and migration between regions was held constant at 50%.

2.3. Model evaluation

2.3.1. Output

The output metrics of interest were classified at individual- and population-level scales. Each simulation of a scenario was run with identical stochastic perturbations (in recruitment and prey biomass) as the base model, and we evaluated the difference between the two models. As an individual-scale response metric, we calculated the mean percent increase in weight-at-age (Δw) during the pulse years, defined as:

$$\Delta w = 0.2 \sum_{y*} \frac{w_{y*,a,s=4,r=1}^{scen} - w_{y*,a,4,1}^{base}}{w_{y*,a,4,1}^{base}} \times 100 \qquad (2)$$

where $y*$ are the years in which a prey pulse occurred, $w_{y*,a,s=4,r=1}^{scen}$ is the weight-at-age of fish in years $y*$ in season 4 and region 1 for either a simulated scenario (*scen*) or for the base model (*base*), and the coefficient 0.2 represents the inverse of the number of years in which a pulse occurred ($1/n_{pulse}$). In this fashion, we isolated the change in mean individual body size that was solely due to the change in prey availability. As population-scale metrics, we calculated the mean percent increase in the spawning stock biomass (ΔS), the annual fishery yield (ΔY), and the following year's recruitment (ΔR) using Eq. (2), but substituting $S_{y*,s'}$, Y_{y*}, and $\sum_r R_{y*+1,r}$ for $w_{y*,a,4,1}$ respectively. Annual fishery yield (Y_y) was calculated as the sum of all catches across seasons, regions, and ages, using Baranov's catch equation (Eq. (T2.11)).

To assess the influence of the prey pulses on achieving management rebuilding goals, we calculated the percent decrease in the time needed to achieve S_{MSY} (Δt) as:

$$\Delta t = \frac{t_{rebuild}^{base} - t_{rebuild}^{scen}}{t_{rebuild}^{base}} \times 100 \qquad (3)$$

where $t_{rebuild}$ is the rebuilding time (yrs) needed for a depleted population to reach S_{MSY} following a reduction in F for either a simulated scenario (*scen*) or for the base model (*base*). For this metric, examined scenarios were restricted to combinations of the three prey pulse scenarios, the three non-constant F sub-scenarios (D, D2, and M), and the migration sub-scenario. Larger Δt values indicate that S_{MSY} was attained more rapidly in the scenario compared to the base model.

The stochastic simulation model was run 1000 times for each unique combination of scenarios. The output metrics are presented as boxplots depicting the distribution of values across the 1000 simulation runs. Cumulative frequency plots of $t_{rebuild}$ across the
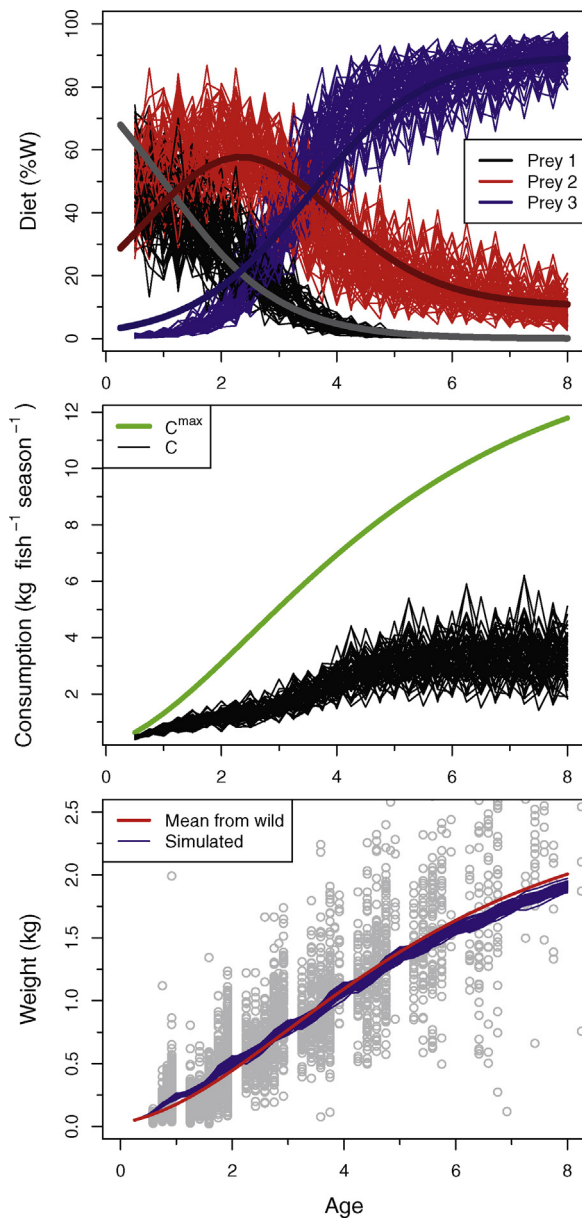
Fig. 2. Growth, consumption, and diet output from one stochastic 80-year run of the base simulation model for summer flounder. (A) Diet composition by age for each simulated year with line color indicating the three different prey types (see legend). The smooth, thick, overlaid lines represent the generalized, empirical patterns in diet composition that were used for model calibration. (B) Per capita seasonal consumption for simulated cohorts (C – black lines) relative to the maximum consumption (C^{max} – green line). (C) Weight-at-age data for wild summer flounder (gray points) with mean empirical growth curve (red line) and simulated cohort growth curves (blue lines) overlaid. (For interpretation of the references to color in this figure legend, the reader is referred to the web version of this article.)

1000 simulation runs were also used to quantify the probability of reaching S_{MSY} based on the number of years following the reduction in F. We ran all models for 80 years, with the first 25 years as a burn-in period. Prey pulses occurred randomly from years 26–50, and the final 30 years allowed for the population to equilibrate.

2.3.2. Sensitivity

The sensitivity of the model output was investigated using two approaches. First, we used a Monte-Carlo sensitivity approach. We ran 1000 simulations in which all parameter values were simultaneously and randomly varied (uniformly within 20% of their defaults) to examine the influence of parameter uncertainty and
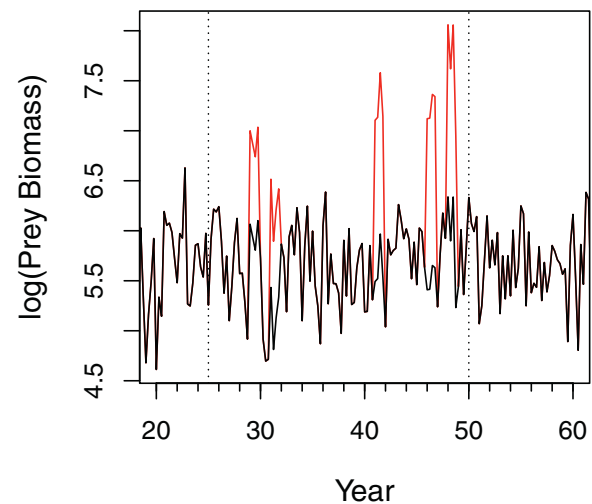
Fig. 3. Prey biomass time-series (kmt) for a base model run (black line) and a prey pulse scenario (red line) whereby base values are multiplied 2–6-fold for five randomly selected years between years 25 and 50 (dotted lines). (For interpretation of the references to color in this figure legend, the reader is referred to the web version of this article.)

potential parameter interactions on the model results and conclusions. Second, to evaluate the relative sensitivity to each model parameter, we re-ran the simulation 100 times after increasing or decreasing an individual parameter by 20%. This was done repeatedly for each parameter, holding all of the other values at their default values. For the ψ values, the default range of a 2–6-fold increase in production was modified to be either a 2–4-fold or a 4–6-fold increase in production. We calculated the mean difference of each output metric (Δw, ΔS, ΔY, ΔR, Δt) from the default scenario models, restricting the models to the decreasing fishing sub-scenario (D) and migration sub-scenarios.

3. Results

The calibrated base model reproduced the mean weight-at-age of wild summer flounder and the general dietary trends with relatively high precision. Temporal stochasticity in prey biomasses generated variability in the dietary composition of simulated fish (± 10–20%; Fig. 2A) as seen in normal conditions in the field; however, simulated prey compositions deviated slightly from the generalized patterns for predators less than age-2 due to the challenge of calibrating the functional response parameters to match the expected diet composition across all ages. Seasonal consumption by predator age did not attain the maximum value, but averaged 28–73% of the maximum consumption, which are reasonable values based on bioenergetics studies for other fishes (Fig. 2B; Hartman and Brandt, 1995b; Stevens et al., 2006). These patterns in consumption-at-age translated into weight-at-age trajectories that corresponded strongly with mean empirical values from the field (Fig. 2C), suggesting that the consumption and growth models generated reasonable results.

3.1. Scenario results

Pulses in prey production were utilized by predators and increased their weight-at-age to varying degrees (Fig. 4). Patterns in the percent increase in weight-at-age followed trends in dietary composition (Fig. 2A); the weight of an age-class increased the most when its most-consumed prey experienced a pulse in production. During pulse years, pulses in prey 1 generated median increases in weight of 16–18% for age-0 and age-1 fish and declined for older age classes (Fig. 4). Pulses in prey 2 caused a median peak

Weight–at–age change (pulse years, mig, decrF)
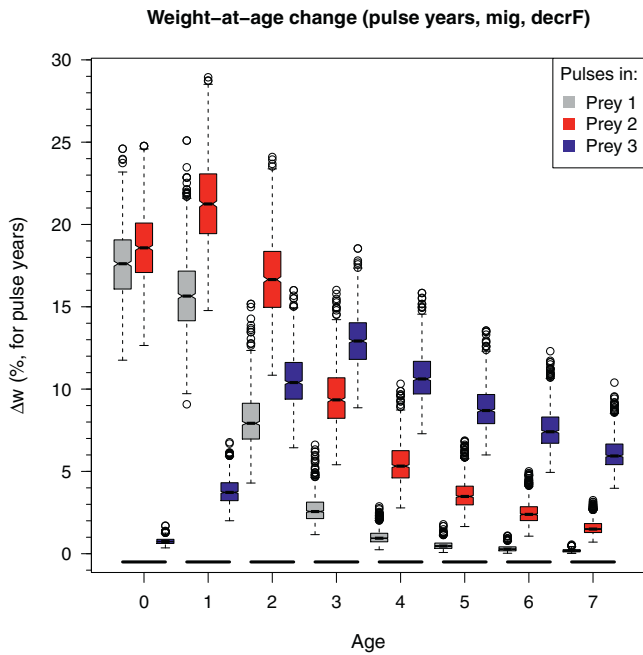
Fig. 4. Percent increase in weight-at-age (Δw) of simulated populations experiencing pulses in prey production relative to the base model populations that experience no pulse. At each age, boxplots are staggered for each of the prey pulse scenarios (prey 1 – gray; prey 2 – red; prey 3 – blue). Boxplots show the distribution of mean values across 1000 stochastic simulation runs (colored bar – interquartile range, horizontal line – median, notches – approximate 95% confidence interval for the median, whiskers – furthest value from the quartile within $1.5\times$ (interquartile range), individual points – outliers). (For interpretation of the references to color in this figure legend, the reader is referred to the web version of this article.)

increase of 21% in weight of age-1 fish with a subsequent decline. Prey 3 pulses generated a median peak of 13% at age-3 and slowly tapered off at older sizes. The relatively large increases in weight-at-age generated by prey pulses were well within the range of observed body sizes from wild fish suggesting that such changes in

Fastest growing pulse cohorts
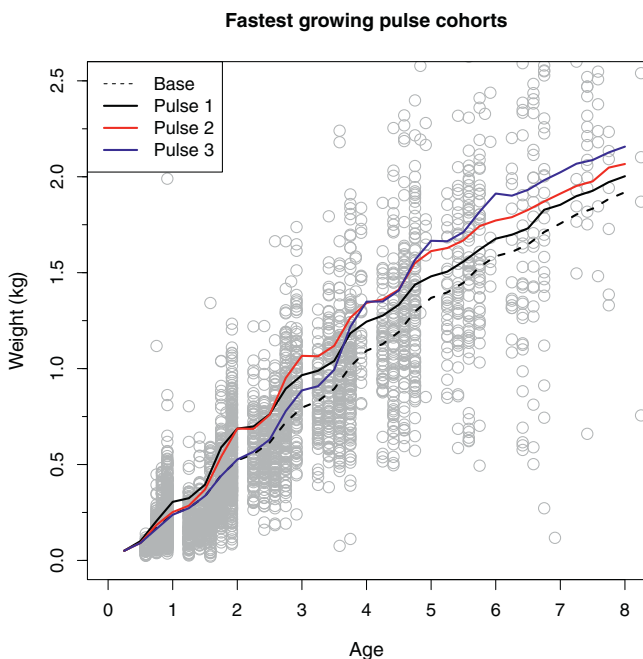
Fig. 5. Simulated growth trajectories for the single fastest-growing cohorts, from all model runs, for each of the pulse scenarios (see legend). Mean growth of all base runs (see legend) and empirical weight-at-age data(points) also presented. Simulations used a migration sub-scenario with a constant, high fishing mortality (fishing sub-scenario H).
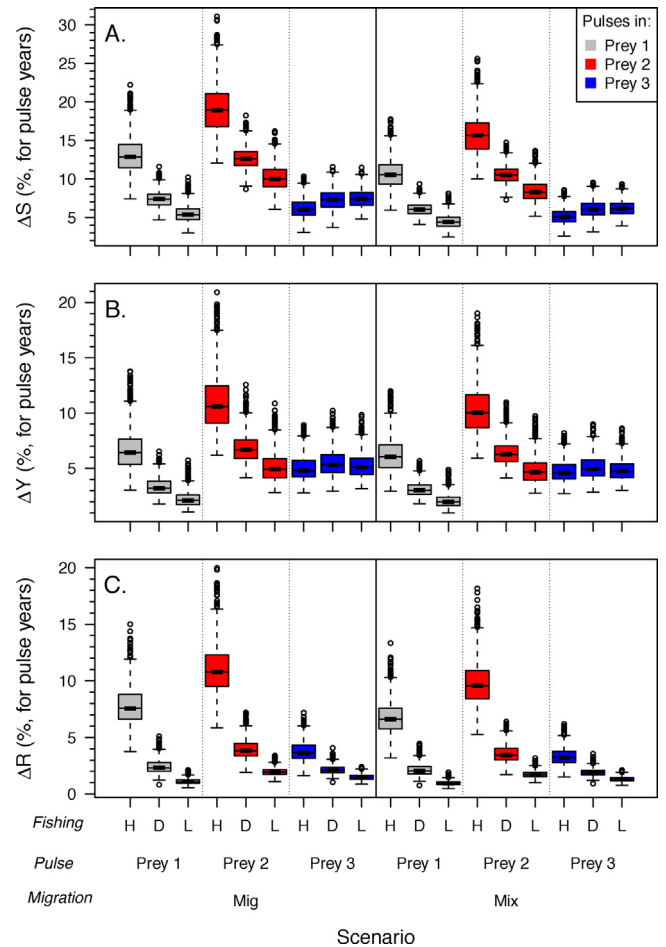

Fig. 6. Population-scale output metrics of simulated summer flounder (*Paralichthys dentatus*) populations. Percent increase in the (A) spawning stock biomass (ΔS), (B) fishery yield (ΔY), and (C) following year's recruitment (ΔR) for various scenarios were calculated relative to base model runs. Scenarios were comprised of different combinations of fishing mortality trends (high – H; decreasing – D; low – L), prey pulses (prey 1 – gray; prey 2 – red; prey 3 – blue), and movement patterns (migration – Mig; fully mixed – Mix). See Fig. 4 for boxplot description. (For interpretation of the references to color in this figure legend, the reader is referred to the web version of this article.)

weight are feasible in natural environments (Fig. 5). The model also reproduced the seasonality in growth patterns that are observed for summer flounder and other fishes (Fig. 5; Powell, 1982). The fully mixed sub-scenario generated nearly identical trends to the migration sub-scenario presented, although the magnitudes of the increases were lower (by as much as 8%). Fishing sub-scenarios had no effect on weight-at-age changes because there were no density-dependent controls on individual growth.

The patterns in the three population-scale metrics (ΔS, ΔY, and ΔR) were similar across the simulated scenarios, although the magnitudes varied (Fig. 6). Relative to the base model, the simulated scenarios generated median increases in S, Y, and R as high as 19%, 11%, and 11% respectively. Generally, ΔS values were higher than ΔY or ΔR. In comparing across the prey scenarios, pulses in prey 2 consistently yielded stronger increases in ΔS, ΔY, and ΔR (with medians up to 13% higher) relative to pulses in prey 1 and 3, regardless of the fishing or movement sub-scenarios. However, an interaction between the effect of prey pulses and fishing pressure was observed; prey 1 pulses generated greater increases in S, Y, and R than prey 3 pulses in the high F sub-scenario, yet the opposite was true for the low F sub-scenario. The two movement sub-scenarios demonstrated that median increases in S for a given
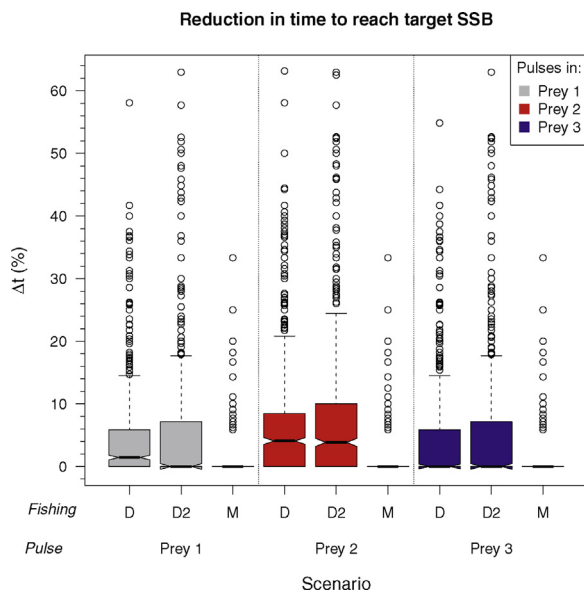
Fig. 7. Percent decrease in the time (Δt) needed for simulated depleted populations to rebuild to target spawning stock biomass, relative to the base model. Scenarios were comprised of different combinations of fishing mortality trends (decreasing – D; rapid decrease – D2; and moratorium – M) and prey pulses (prey 1 – gray; prey 2 – red; prey 3 – blue). Results plotted for the migration sub-scenario only. See Fig. 4 for boxplot description. (For interpretation of the references to color in this figure legend, the reader is referred to the web version of this article.)

prey pulse were only slightly greater (0.9–3.3%) for the migration sub-scenario relative to the fully mixed scenario.

The influence of the different prey pulses on the recovery time of the overfished stock was highly variable, yielding 0–63% reductions in $t_{rebuild}$ (Fig. 7). The median declines in $t_{rebuild}$ for the prey 1 and prey 3 pulse scenarios were 0–1% and the declines were modest for pulses in prey 2 (4%, or 1 year). However, reductions in $t_{rebuild}$ of 10% were not uncommon across scenarios. The largest outliers occurred in simulations where a prey pulse increased S sufficiently to achieve S_{MSY} prior to a random period of poor recruitment that otherwise maintained the base model run below S_{MSY} for an extended length of time (Fig. A2).

Expressing $t_{rebuild}$ values as cumulative probabilities demonstrated the relatively modest declines in $t_{rebuild}$ that resulted from pulses in prey production compared to the different implementations of fishing mortality controls (Fig. 8). For example, prey pulses in fishing sub-scenario D increased the probability of achieving S_{MSY} within 14 years by only ~3–6.5% relative to that sub-scenario's base run; in contrast, a more stringent implementation of fishing controls (i.e., base run of sub-scenario D2) would increase the probability of achieving S_{MSY} by 41% over the probability of success with the base run of sub-scenario D. Under the moratorium fishing sub-scenario (M), prey pulses exhibited no detectable effect on achieving the management target. Under moratorium there was a 50% probability of rebuilding the stock within 4–5 years, compared to 14 and 18 years for the same probability benchmark under the D2 and D base scenarios, respectively.

3.2. Sensitivity results

Simulation outputs were not overly sensitive to the choice of parameter values. Monte-Carlo sensitivity runs generated similar patterns in Δw, ΔS, ΔY, and ΔR to those presented in Figs. 4 and 6, although the variability across simulations increased (~2-fold increase in the interquartile spread), and the median responses tended to decrease slightly (Figs. A3 and A4). Based on perturbations of individual parameters (Fig. A5), Δw, ΔS, and ΔY were most
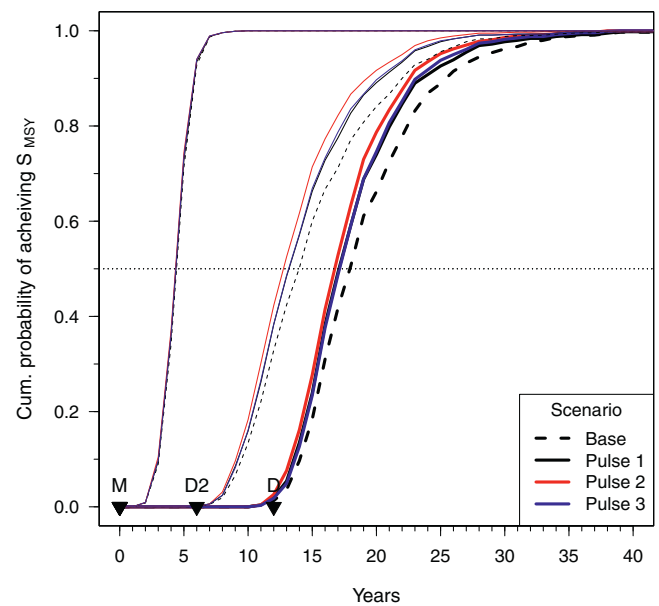
Fig. 8. Cumulative probability of achieving the target spawning stock biomass (S_{MSY}) under different simulated pulse and fishing scenarios. Prey pulse scenario is indicated by line type relative to its base model (see legend). Each group of curves reflects a different fishing mortality sub-scenario (moratorium – M, rapid decrease – D2, decrease – D), with black triangles marking the year in which the target F (F_{MSY}) was achieved for each F sub-scenario.

sensitive to prey biomass and consumption parameters (specifically ψ, $\bar{N}_2$, η_3, and CTO), whereas ΔR was most sensitive to parameters of population dynamics (α_{SR}, β_{SR}, M), prey biomass time series (ψ, $\bar{N}_2$), and growth (KL, KR, KW, CTO). However, Δw, ΔS, ΔY, and ΔR typically varied by no more than $\pm 3\%$ due to the parameter perturbations. The Δt estimates were most sensitive to growth (KL, KR, KW, CQ, CTO), population dynamics (α_{SR}, β_{SR}, κ_{SR}, M), and prey biomass ($\bar{N}_2$, σ_γ, n_{pulse}) parameters. Perturbations of these parameters for the pulse in prey 2 scenario resulted in median differences in Δt of –5% (Fig. A5); in other words, shifting these parameters by 20% yielded no median change in the time to rebuild when comparing a pulse in prey 2 scenario and the base model.

4. Discussion

In this study, we used a mechanistic predator–prey simulation model to evaluate the population-scale consequences of episodic increases of prey production that occur in the wild. The simulation model demonstrated the substantial bottom-up effects that prey pulses can have on the growth, production, and reproductive numerical response of a predator. Predator gains in growth and production were not equivalent across prey pulses with results suggesting that increases in production of small forage fishes, rather than in crustacean or large fish prey, may be more beneficial to predators like summer flounder. Fishing pressure (i.e., top-down control) mediated the strength of the predator's numerical response to increased prey production by altering spawning stock biomass and the resulting density-dependent recruitment. Prey pulses did not substantially alter the rebuilding timelines for recovering populations, highlighting the stronger influences of fishing and recruitment variability on stock rebuilding. Population responses to the interactive effects of bottom up and top down effects are difficult to detect in natural settings due to environmental variability and predator–prey dynamics, but simulation modeling provides a valuable tool for exploring these ecological processes.

Patterns in the population-scale responses to prey pulses integrated the individual growth response with population mortality

losses and reproductive additions. Physiologically, younger fish have a greater scope for growth facilitating larger proportional increases in weight-at-age than older conspecifics (Brett and Groves, 1979); however this did not necessarily correspond to greater increases in S, Y, and R. The scaling of the weight-at-age responses to the population-level relied on integrating these biomass gains demographically across ages, while partitioning the predatory production gains to natural mortality, fishing, or spawning stock biomass accumulation. Although some prey groups such as mysids and small crustaceans (prey 1) generated relatively strong increases in weight-at-age, these gains were constrained to a more narrow age range than the other prey, and a greater proportion of this production was lost through natural mortality before fish could mature to contribute to increased S and R. Increased production of small forage fishes (prey 2) translated into the largest increases in S, Y, and R because young predators exhibited greater growth, the prey was consumed over a broader range of ages, and many of these fish matured and spawned prior to becoming vulnerable to fishing. Overall, this suggests that the magnitude of bottom-up effects on predatory production reflects a balance between the predator's growth potential (with greater scope at smaller sizes) and the total dietary contribution across age classes; increased production is then routed to natural mortality losses, fishery removal, or S accumulation based on the rates of mortality, fishing, and maturation.

Top-down pressure on the predator population, in the form of fishery removals, affected the capacity of the population to respond to the resource-driven, bottom-up forcing. Similar interactions between bottom-up and top-down forces are common in natural ecosystems and demonstrate the dynamic nature of ecosystem structure and control (Hunter and Price, 1992; Hunt and McKinnell, 2006). In our model, this interaction was caused by the density-dependent processes underlying the SR function. By maintaining S at lower levels, higher fishing rates produced stronger population compensation whereby the recruits per spawner was larger (Rose et al., 2001), thus facilitating greater increases in S and R within prey 1 and prey 2 pulse scenarios. In the prey 3 pulse scenario with high F, the additional predatory production was shunted more to the fishery restricting the accumulation of S, but R still increased (relative to the decreasing and low fishing rate scenarios) due to compensation. Thus, top down fishing pressure can influence a population's ability to capitalize on bottom-up forcing by regulating the density-dependent production (i.e., compensation) expected at lower stock sizes.

Recruitment is one of the most critical processes regulating population dynamics, but it remains challenging to predict given the complex interactions among various density-independent and density-dependent factors that govern recruitment strength (Sissenwine, 1984; Houde, 2009). The reproductive numerical response in this simulation model relied on the density-dependent nature of the SR function, but it was not overly sensitive to the parameterization of the SR function. Although summer flounder recruitment data can appear independent of S (Maunder, 2012), the empirical realization of an underlying density-dependent relationship is obscured by large natural variability in recruitment, in addition to sampling and estimation errors of those values. In our simulations, we could rely on broader theoretical and empirical support for compensatory mechanisms operating on fish populations (Rose et al., 2001), while also standardizing and accounting for uncertainty through the inclusion of the stochastic recruitment deviations. Summer flounder and other flatfishes have relatively high steepness values for SR relationships (Maunder, 2012; steepness = 0.74 in this study) indicating that recruitment remains relatively high at low S compared to other commercial species (Myers et al., 1999; Rose et al., 2001). Therefore, other species with lower steepness could be expected to exhibit stronger

proportional increases in R and S due to prey pulses, given similar conditions to our simulation.

From a fisheries management perspective, the numerical responses of predators to increases in prey production had relatively minor effects on rebuilding times relative to recruitment variability and fishing pressure. Recruitment stochasticity, which represented various climatic, oceanographic, and ecological processes known to influence recruitment (Houde, 2009), generated far greater variability in rebuilding time than prey pulses alone. The role of strong recruitment years can facilitate the recovery of overfished stocks (Richards and Rago, 1999; Hart and Rago, 2006), but in the wild any numerical responses of the form we have investigated would be embedded within a complex mosaic of environmental and biological controls on recruitment. However, our simulations emphasized the predominant role that curbing top-down fishing pressure has on the speed at which target stock sizes are attained (Safina et al., 2005; Rosenberg et al., 2006). Given the greater accumulation of S and stronger reproductive numerical responses of predators to pulses in prey 1 and 2 (at high F), conservation of prey for younger age-classes of an overfished predatory stock could provide some benefits for rebuilding the population. But, one important caveat is that our simulation assumed that none of the prey resources were severely depleted or limiting. For example, if prey 3 represented a depleted forage fish population, then that trophic linkage could be a bottleneck for predator nutrition, preventing suitable growth and stock recovery (e.g., Hartman and Margraf, 2003).

The movement patterns of the simulated population influenced the degree of spatial-temporal overlap of predators with the spatially constrained pulses in prey production. A fully mixed population was less able to capitalize on improved foraging conditions in the nearshore environment. The availability of diverse and abundant prey resources within estuarine and nearshore habitats is an important component selecting for the estuarine-dependent life history strategies of summer flounder and many other coastal fishes (Beck et al., 2001; Able, 2005). Although summer flounder are managed as a unit stock in the northwest Atlantic, as many as three sub-populations have been proposed to exist within the stock area (Terceiro, 2002). In cases of increased spatial structure among subpopulations, we would anticipate any reproductive numerical responses of the population to be similarly controlled by the extent of spatiotemporal overlap of predators with areas of increased prey productivity but potentially modified by any spatial patterns in fishing.

The level of complexity for the simulation model was chosen to simplify the mechanistic processes governing consumption, growth, and population dynamics while accounting for the major factors of influence and representing empirical data. For example, our simple consumption and growth models accounted for the effects of temperature, prey availability, predator size, and diet ontogeny, which rank as some of the most dominant regulators of prey consumption and growth (Brett and Groves, 1979). Any effects resulting from differences in prey quality were assumed to be minimal given the similarity in energy densities (within 10%) among summer flounder and representative species from the three prey groups (Hartman and Brandt, 1995b; Horodysky and Schloesser, unpublished data). For the multispecies functional response, there was insufficient empirical data to adequately parameterize the model, as is typically the case for predator–prey models at large spatial scales (Hunsicker et al., 2011). While the absolute values of the parameters used in the functional response model may not be accurate for the wild population, the relative attack rates and relative biomasses defined predator–prey dynamics that successfully represented empirical patterns in weight-at-age and diet composition with reasonable levels of total consumption relative to C^{max}.

Four model assumptions could potentially have a larger influence on the model dynamics and our conclusions. First, we assumed that the predator–prey system was adequately described using three prey groups. Marine food webs can be highly complex and connected, characterized by a multitude of trophic linkages and high degree of omnivory (Link, 2002). However, trophic complexity is reduced when prey are aggregated into size or functional groups as we have done (French et al., 2013), and omnivory and prey switching was incorporated at this coarse resolution of prey (with the multi-species functional response). Second, although our assumption that predators have negligible effects on prey dynamics is supported for our modeled species (see Section 2.1.3), predator–prey feedbacks would be an important consideration for systems with stronger interactions or evidence of top-down trophic cascades. Third, our model formulation did not account for any indirect effects among the modeled groups (e.g., pulses affecting other prey groups and their predators), assuming that these effects would be minimal and potentially delayed relative to the modeled direct effects. Fourth, we assumed that natural mortality was constant as commonly employed in population models and stock assessments (e.g., Terceiro, 2011). However, improved foraging and growth can alter mortality rates and can be part of the mechanism regulating recruitment strength and reproductive numerical responses (Cushing, 1990; Houde, 2009). These foraging effects on survival appear most drastic and notable on early life history (i.e., larval and early juvenile) stages of fishes (Sissenwine, 1984; Caddy, 1991), therefore the majority of this effect would occur prior to the initiation of our predator population at 3 months of age. Generally, there is limited empirical, quantitative information to parameterize the ecological regulation of natural mortality across ages at the population-scale (e.g., Caddy, 1991; Maunder and Wong, 2011), therefore we were unable to justify the form and magnitude of any effects of prey pulses and improved growth on natural mortality. Consequently, we consider our estimates to be conservative measures of the effects that pulses in prey production have on a predator population, with regards to our natural mortality assumption.

Age-specific predator–prey models like the one developed here provide a simple framework for testing the effects of bottom-up and top-down influences on a predator population. Given that ecosystem approaches to fisheries management ideally rely on a blend of model types (Link, 2010a), this age-specific approach can complement more complex ecosystem models. Ecosystem models can provide a broader assessment of system-wide consequences (both direct and indirect) of changes in production or fishing, but they do not typically provide high ontogenetic resolution within modeled species groups. As shown in our study, the ontogenetically variable feeding habits of fishes have bearing on the individual- and population-scale responses of predators to bottom-up forcing, particularly for species with varying degrees of historical fishing pressure (Hunt and McKinnell, 2006). In the simulations, depleted populations were the most sensitive to episodic pulses in prey production, but detection of such effects would be easily obscured in wild populations due to other factors influencing recruitment variability which is particularly high at low stock sizes (Myers, 2001). While these bottom-up effects of prey pulses can benefit rebuilding plans of overfished populations, their small magnitude relative to changes in fishing mortality supports the primacy of regulating fishing for stock recovery.

## Acknowledgments

Appendix.

See Table A1 and Figs. A1–A5.

Table A1
Parameter values for the base simulation model. See Tables 1 and 2 for symbol definitions and model equations.

| Symbol	Parameter value	Sources
$\phi_{s,n\to r}$	$\phi_{s,1\to 2}$ = 0.0, 0.0, 0.4, 0.9	Packer et al. (1999), Terceiro (2002)
$\phi_{s,r\to n}$	$\phi_{s,2\to 1}$ = 0.3, 0.95, 0.0, 0.0	Packer et al. (1999), Terceiro (2002)
F_y	See F scenarios	Terceiro (2011)
sel_a	sel_a = 0.0, 0.1, 0.5, 1, 1, 1, 1, 1	Terceiro (2011)
M	0.25	Terceiro (2011)
α_{SR}	3.4	Rothschild et al. (2012)
κ_{SR}	27	Rothschild et al. (2012)
β_{SR}	1	Rothschild et al. (2012)
θ_r	θ_1 = 0.9, θ_2 = 0.1	Assumed
δ_y	σ_δ = 0.4	Terceiro (2011)
$m_{a,s'}$	$m_{a=0-3+}$ = 0.38, 0.72, 0.90, 1.0	Terceiro (2011)
w_0	0.051	Buchheister (unpublished)
KL	0.5	Optimized
KR	−0.0014	Optimized
KW	−600	Optimized
h	1	Assumed, corresponds with a Type-II functional response
λ_j	$\lambda_1 = e^{-19.5}$, $\lambda_2 = e^{-16.3}$, $\lambda_3 = e^{-13.5}$	Optimized
ρ_j	ρ_1 = −1.1, ρ_2 = 0.46, ρ_3 = 1.9	Optimized
η_j	η_1 = 2, η_3 = 3.5	Assumed, based on survey diet data (ChesMMAP, NEAMAP)
η_{1j}, η_{2j}	1, 4	Assumed, based on survey diet data (ChesMMAP, NEAMAP)
CA	0.3	Modified from Hartman and Brandt (1995a,b)
CB	−0.2	Modified from Hartman and Brandt (1995a,b)
$\bar{N}$	3×10^{10}	Jung and Houde (2004a)
τ_j	τ_1 = 10, τ_3 = 0.1	Assumed, based on Link (2010b)
$\psi_{y,r}$	$\psi_{y^*,1}$ = U(2, 6); otherwise ψ = 1	Assumed
σ_γ	σ_γ = 0.4	Assumed
$T_{s,r}$	$T_{s,1}$ = 4.4, 13.6, 24.4, 14.8; $T_{s,2}$ = 7.6, 10.8, 13.5, 15.2	Chesapeake Bay Program and NEFSC databases
CTM	35	Modified from Burke and Rice (2002)
CTO	22	Modified from Burke and Rice (2002)
CQ	2.5	Modified from Burke and Rice (2002)
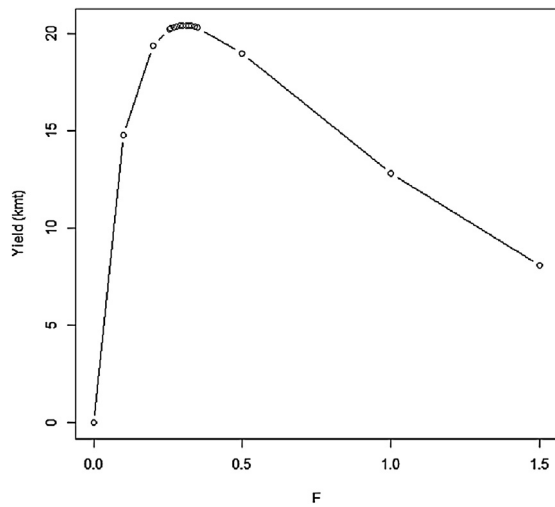
Fig. A1. Sustainable fishery yield (kmt) at varying levels of instantaneous fishing mortality (*F*). Results were generated from the simulation model with all stochasticity removed. Maximum sustainable yield (MSY) was achieved at $F_{MSY} = 0.31$.
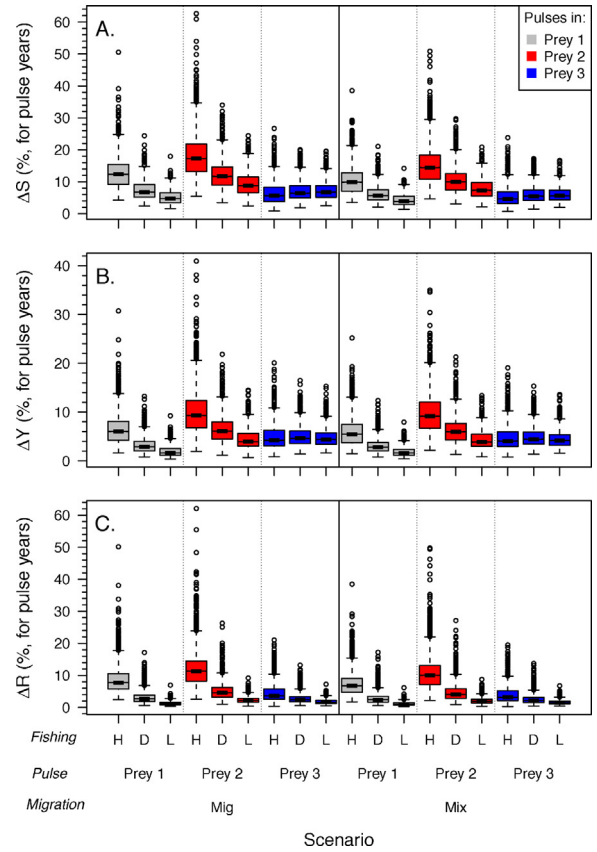

Fig. A3. Monte-Carlo sensitivity results for population-scale output metrics of simulated summer flounder (*Paralichthys dentatus*) populations. Percent increase in the (A) spawning stock biomass (ΔS), (B) fishery yield (ΔY), and (C) following year's recruitment (ΔR) for various scenarios were calculated relative to base model runs. Scenarios were comprised of different combinations of fishing mortality trends (high – H; decreasing – D; low – L), prey pulses (prey 1 – gray; prey 2 – red; prey 3 – blue), and movement patterns (migration – Mig; fully mixed – Mix), with model parameters randomly selected within ±20% of default values. See Fig. 4 for boxplot description. (For interpretation of the references to color in this figure legend, the reader is referred to the web version of this article.)
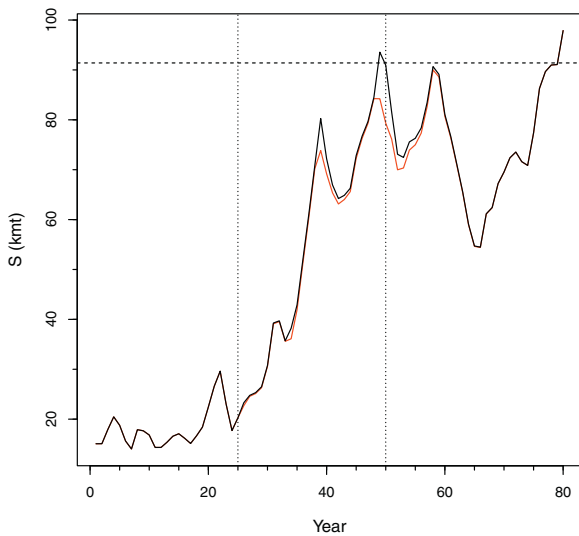
Fig. A2. Recovery of spawning stock biomass (*S*) for a simulated population under the decreasing fishing mortality sub-scenario. This outlier simulation run yielded a large difference in the time to reach S_{MSY} (horizontal dashed line) between a pulse scenario (black line) and the base model (red line). Vertical dotted lines denote the start and end of the period in which prey pulses could occur. (For interpretation of the references to color in this figure legend, the reader is referred to the web version of this article.)
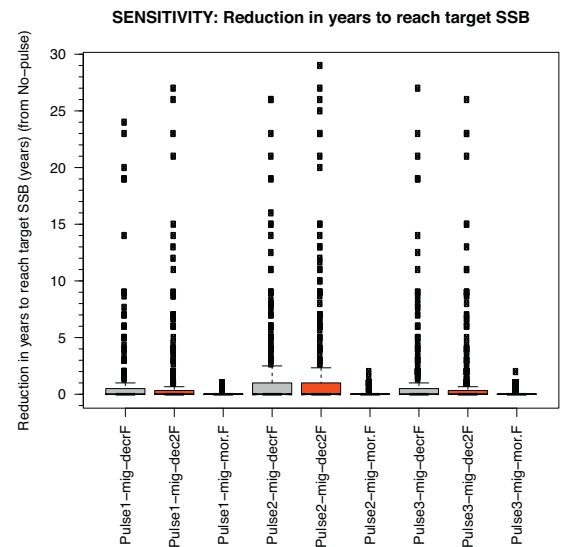
Fig. A4. Monte-Carlo sensitivity results for the difference in rebuilding times (Δt) relative to the base model. Models were run by randomly selecting all parameters within ±20% of default values. Scenarios were comprised of different combinations of fishing mortality trends (decreasing – D; rapid decrease – D2; and moratorium – M) and prey pulses (prey 1 – gray; prey 2 – red; prey 3 – blue). Results were plotted for the migration sub-scenario only. See Fig. 4 for boxplot description. (For interpretation of the references to color in this figure legend, the reader is referred to the web version of this article.)
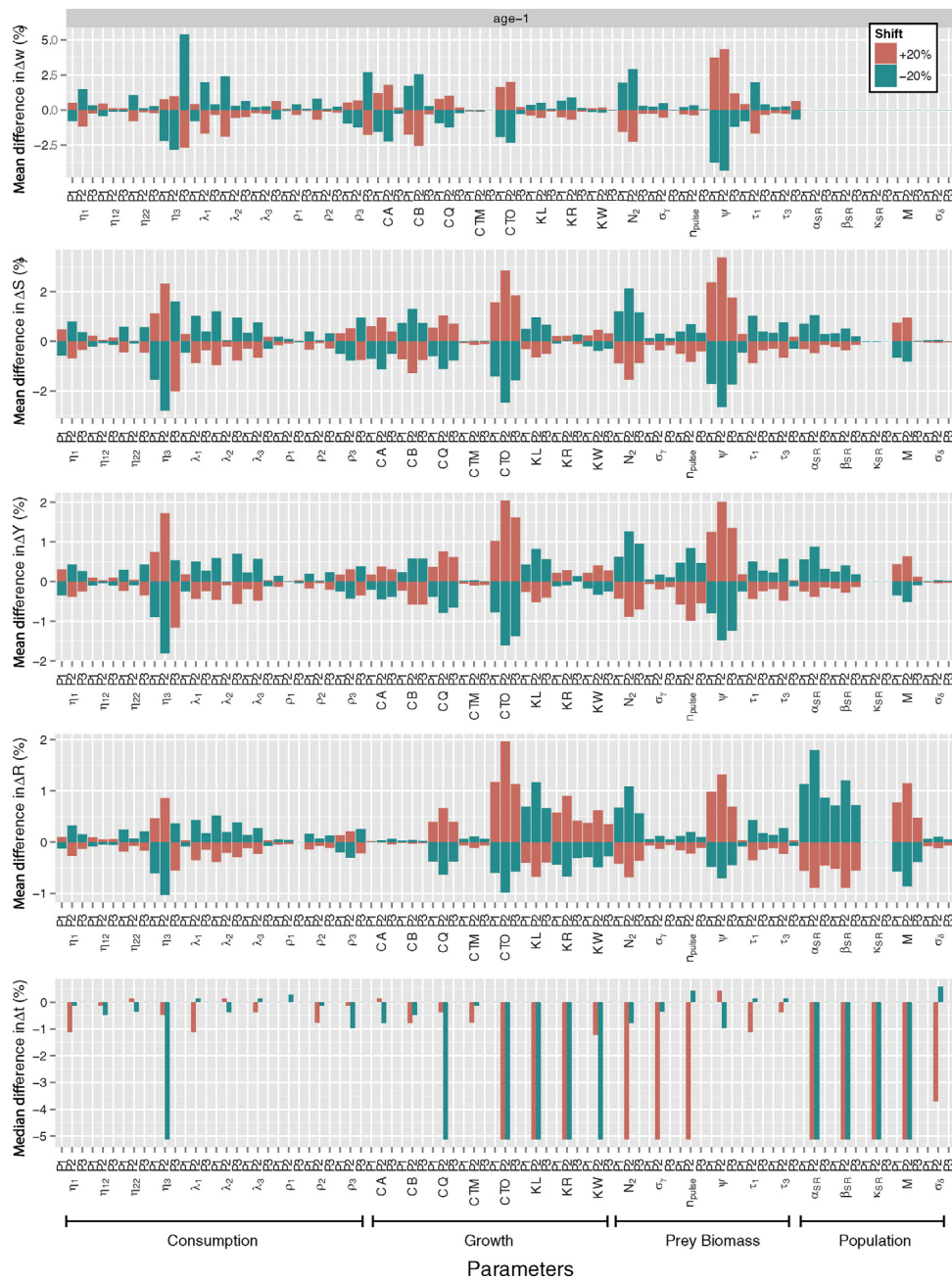
Fig. A5. Sensitivity of model outputs to perturbations of individual model parameters. Each parameter was shifted ±20% (see legend) while holding all other parameters at default values. Mean or median differences in weight-at-age (Δw), spawning stock biomass (ΔS), fishery yield (ΔY), recruitment (ΔR), and rebuilding time (Δt) are presented relative to the standard simulation scenario runs (zero line). Standard simulation scenario runs included pulses in prey 1 (P1), prey 2 (P2), and prey 3 (P3), using the migration and decreasing fishing mortality sub-scenarios. Parameters are grouped based on the process they most directly influence (consumption, growth, prey biomass, or population dynamics). Weight-at-age plot is for age-1 fish which was representative of other age-classes. See Table 1 for parameter definitions. Positive values indicate a stronger effect of a pulse relative to the default simulation.

References

Able, K.W., 2005. A re-examination of fish estuarine dependence: evidence for connectivity between estuarine and ocean habitats. Estuar. Coast. Shelf Sci. 64, 5–17, http://dx.doi.org/10.1016/j.ecss.2005.02.002

Aebischer, N.J., Coulson, J.C., Colebrookl, J.M., 1990. Parallel long-term trends across four marine trophic levels and weather. Nature 347, 753–755, http://dx.doi.org/10.1038/347753a0

Beaugrand, G., Brander, K.M., Alistair Lindley, J., Souissi, S., Reid, P.C., 2003. Plankton effect on cod recruitment in the North Sea. Nature 426, 661–664, http://dx.doi.org/10.1038/nature02164

Beck, M.W., Heck Jr., K.L., Able, K.W., Childers, D.L., Eggleston, D.B., Gillanders, B.M., Halpern, B., Hays, C.G., Hoshino, K., Minello, T.J., Orth, R.J., Sheridan, P.F., Weinstein, M.P., 2001. The identification, conservation, and management of estuarine and marine nurseries for fish and invertebrates. Bioscience 51, 633–641, http://dx.doi.org/10.1641/0006-3568(2001)051

Bonzek, C.F., Gartland, J., Latour, R.J., 2011. Data Collection and Analysis in Support of Single and Multispecies Stock Assessments in Chesapeake Bay: The Chesapeake Bay Multispecies Monitoring and Assessment Program. Rep. to VA Mar. Resour. Comm. U.S. Fish Wildl. Serv., pp. 1–155.

Brett, J.R., 1979. Environmental factors and growth. In: Hoar, W.S., Randall, D.J., Brett, J.R. (Eds.), Fish Physiology, vol. 8. Academic Press, New York, pp. 599–677.

Brett, J.R., Groves, T.D.D., 1979. Physiological energetics. In: Hoar, W.S., Randall, D.J., Brett, J.R. (Eds.), Fish Physiology, vol. 8. Academic Press, New York, pp. 279–352.

Buchheister, A., Latour, R.J., 2011. Trophic ecology of summer flounder in lower Chesapeake Bay inferred from stomach content and stable isotope analyses. Trans. Am. Fish. Soc. 140, 1240–1254.

Buchheister, A., Latour, R.J., 2015a. Diets and trophic guild structure of a diverse fish assemblage in Chesapeake Bay, USA. J. Fish. Biol. 86, 967–992.

Buchheister, A., Latour, R.J., 2015b. Dynamic trophic linkages in a large estuarine system – support for supply-driven dietary changes using delta generalized additive mixed models. Can. J. Fish. Aquat. Sci. (in press).

Burke, B.J., Rice, J.A., 2002. A linked foraging and bioenergetics model for southern flounder. Trans. Am. Fish. Soc. 131, 120–131.

Caddy, J.F., 1991. Death rates and time intervals: is there an alternative to the constant natural mortality axiom? Rev. Fish Biol. Fish. 1, 109–138, http://dx.doi.org/10.1007/BF00157581

Castonguay, M., Plourde, S., Robert, D., Runge, J.A., Fortier, L., 2008. Copepod production drives recruitment in a marine fish. Can. J. Fish. Aquat. Sci. 65, 1528–1531, http://dx.doi.org/10.1139/F08-126

Chavez, F.P., Ryan, J., Lluch-Cota, S.E., Niquen, M., 2003. From anchovies to sardines and back: multidecadal change in the Pacific Ocean. Science 299, 217–221.

Christensen, V., Beattie, A., Buchanan, C., Ma, H., Martell, S.J.D., Latour, R.J., Preikshot, D., Sigrist, M.B., Uphoff, J.H., Walters, C.J., Wood, R.J., Townsend, H., 2009. Fisheries Ecosystem Model of the Chesapeake Bay: Methodology, Parameterization, and Model Exploration. U.S. Department of Commerce, NOAA Technical Memorandum NMFS-F/SPO, pp. 1–146.

Closs, G.P., Balcombe, S.R., Shirley, M.J., 1999. Generalist predators, interaction strength and food-web stability. Adv. Ecol. Res. 28, 93–126.

Cury, P., Shannon, L., 2004. Regime shifts in upwelling ecosystems: observed changes and possible mechanisms in the northern and southern Benguela. Prog. Oceanogr. 60, 223–243, http://dx.doi.org/10.1016/j.pocean.2004.02.007

Cushing, D.H., 1990. Plankton production and year-class strength in fish populations: an update of the match/mismatch hypothesis. Adv. Mar. Biol. 26, 249–293.

Frank, K.T., Petrie, B., Shackell, N.L., 2007. The ups and downs of trophic control in continental shelf ecosystems. Trends Ecol. Evol. 22, 236–242.

Frederiksen, M., Edwards, M., Richardson, A.J., Halliday, N.C., Wanless, S., 2006. From plankton to top predators: bottom-up control of a marine food web across four trophic levels. J. Anim. Ecol. 75, 1259–1268, http://dx.doi.org/10.1111/j.1365-2656.2006.01148.x

French, B., Clarke, K.R., Platell, M.E., Potter, I.C., 2013. An innovative statistical approach to constructing a readily comprehensible food web for a demersal fish community. Estuar. Coast. Shelf Sci. 125, 43–56, http://dx.doi.org/10.1016/j.ecss.2013.03.014

Gjøsæter, H., Bogstad, B., Tjelmeland, S., 2009. Ecosystem effects of the three capelin stock collapses in the Barents Sea Ecosystem effects of the three capelin stock collapses in the Barents Sea. Mar. Biol. Res. 5, 40–53, http://dx.doi.org/10.1080/17451000802454866

Hanson, P.C., Johnson, T.B., Schindler, D.E., Kitchell, J.F., 1997. Fish Bioenergetics 3.0 for Windows – Users Manual. University of Wisconsin Sea Grant Institute.

Hart, D.R., Rago, P.J., 2006. Long-term dynamics of U.S. Atlantic sea scallop Placopecten magellanicus populations. North Am. J. Fish. Manag. 26, 490–501, http://dx.doi.org/10.1577/M04-116.1

Hartman, K.J., Brandt, S.B., 1995a. Comparative energetics and the development of bioenergetics models for sympatric estuarine piscivores. Can. J. Fish. Aquat. Sci. 52, 1647–1666.

Hartman, K.J., Brandt, S.B., 1995b. Predatory demand and impact of striped bass, bluefish, and weakfish in the Chesapeake Bay: applications of bioenergetics models. Can. J. Fish. Aquat. Sci. 52, 1667–1687.

Hartman, K.J., Margraf, F.J., 2003. US Atlantic coast striped bass: issues with a recovered population. Fish. Manag. Ecol. 10, 309–312.

Holland, A.F., Shaughnessy, A.T., Hiegel, M.H., 1987. Long-term variation in mesohaline Chesapeake Bay macrobenthos: spatial and temporal patterns. Estuaries 10, 227–245.

Holling, C.S., 1959. The components of predation as revealed by a study of small-mammal predation of the European pine sawfly. Can. Entomol. 91, 293–320.

Houde, E.D., 2009. Recruitment variability. In: Jakobsen, T., Fogarty, M., Megrey, B.A., Moksness, E. (Eds.), Reproductive Biology of Fishes: Implications for Assessment and Management. Blackwell Publishing, Malaysia, pp. 91–171.

Hunsicker, M.E., Ciannelli, L., Bailey, K.M., Buckel, J.A., White, W.J., Link, J.S., Essington, T.E., Gaichas, S., Anderson, T.W., Brodeur, R.D., Chan, K.-S., Chen, K., Englund, G., Frank, K.T., Freitas, V., Hixon, M.A., Hurst, T., Johnson, D.W., Kitchell, J.F., Reese, D., Rose, G.A., Sjodin, H., Sydeman, W.J., van der Veer, H.W., Vollset, K., Zador, S., 2011. Functional responses and scaling in predator–prey interactions of marine fishes: contemporary issues and emerging concepts. Ecol. Lett. 14, 1288–1299, http://dx.doi.org/10.1111/j.1461-0248.2011.01696.x

Hunt, G.L., McKinnell, S., 2006. Interplay between top-down, bottom-up, and wasp-waist control in marine ecosystems. Prog. Oceanogr. 68, 115–124, http://dx.doi.org/10.1016/j.pocean.2006.02.008

Hunt, G.L., Stabeno, P.J., 2002. Climate change and the control of energy flow in the southeastern Bering Sea. Prog. Oceanogr. 55, 5–22, http://dx.doi.org/10.1016/S0079-6611(02)00067-8

Hunter, M.D., Price, P.W., 1992. Playing chutes and ladders: heterogeneity and the relative roles of bottom-up and top-down forces in natural communities. Ecology 73, 724–732.

Jung, S., Houde, E., 2004a. Production of bay anchovy Anchoa mitchilli in Chesapeake Bay: application of size-based theory. Mar. Ecol. Prog. Ser. 281, 217–232, http://dx.doi.org/10.3354/meps281217

Jung, S., Houde, E.D., 2004b. Recruitment and spawning-stock biomass distribution of bay anchovy (Anchoa mitchilli) in Chesapeake Bay. Fish. Bull. 102, 63–77.

Koen-Alonso, M., 2007. A process-oriented approach to the multispecies functional response. In: Rooney, N., McCann, K.S., Noakes, D.L.G. (Eds.), From Energetics to Ecosystems: The Dynamics and Structure of Ecological Systems. Springer, New York.

Latour, R.J., Gartland, J., Bonzek, C.F., Johnson, R.A., 2008. The trophic dynamics of summer flounder (Paralichthys dentatus) in Chesapeake Bay. Fish. Bull. 106, 47–57.

Link, J.S., 2002. Does food web theory work for marine ecosystems? Mar. Ecol. Prog. Ser. 230, 1–9.

Link, J.S., 2010a. Ecosystem-Based Fisheries Management: Confronting Tradeoffs. Cambridge University Press, New York.

Link, J.S., 2010b. Adding rigor to ecological network models by evaluating a set of pre-balance diagnostics: a plea for PREBAL. Ecol. Model. 221, 1580–1591, http://dx.doi.org/10.1016/j.ecolmodel.2010.03.012

Link, J.S., Bolles, K., Milliken, C.G., 2002. The feeding ecology of flatfish in the North-west Atlantic. J. Northwest Atl. Fish. Sci. 30, 1–17.

Maunder, M.N., 2012. Evaluating the stock–recruitment relationship and management reference points: application to summer flounder (Paralichthys dentatus) in the U.S. mid-Atlantic. Fish. Res. 125–126, 20–26, http://dx.doi.org/10.1016/j.fishres.2012.02.006

Maunder, M.N., Wong, R.A., 2011. Approaches for estimating natural mortality: application to summer flounder (Paralichthys dentatus) in the U.S. mid-Atlantic. Fish. Res. 111, 92–99, http://dx.doi.org/10.1016/j.fishres.2011.06.016

Mcfarlane, G.A., Beamish, R.J., 1992. Climatic influence linking copepod production with strong year-classes in sablefish, Anoplopoma fimbria. Can. J. Fish. Aquat. Sci. 49, 743–753.

McGowan, J., Cayan, D., Dorman, L., 1998. Climate-ocean variability and ecosystem response in the Northeast Pacific. Science 281, 210–216.

Myers, R., 2001. Stock and recruitment: generalizations about maximum reproductive rate, density dependence, and variability using meta-analytic approaches. ICES J. Mar. Sci. 58, 937–951, http://dx.doi.org/10.1006/jmsc.2001.1109

Myers, R.A., Bowen, K.G., Barrowman, N.J., 1999. Maximum reproductive rate of fish at low population sizes. Can. J. Fish. Aquat. Sci. 56, 2404–2419, http://dx.doi.org/10.1139/f99-201

Packer, D.B., Griesbach, S.J., Berrien, P.L., Zetlin, C.A., Johnson, D.L., Morse, W.W., 1999. Essential Fish Habitat Document: Summer Flounder, Paralichthys dentatus, Life History and Habitat Characteristics. U.S. National Oceanic and Atmospheric Administration, NOAA Technical Memorandum NMFS-NE-151.

Powell, A.B., 1982. Annulus formation on otoliths and growth of young summer flounder from Pamlico Sound, North Carolina. Trans. Am. Fish. Soc. 111, 688–693.

Richards, R.A., Rago, P.J., 1999. A case history of effective fishery management: Chesapeake Bay striped bass. North Am. J. Fish. Manag. 19, 356–375.

Ringuette, M., Castonguay, M., Runge, J.A., Grégoire, F., 2002. Atlantic mackerel (Scomber scombrus) recruitment fluctuations in relation to copepod production and juvenile growth. Can. J. Fish. Aquat. Sci. 59, 646–656, http://dx.doi.org/10.1139/F02-039

Rose, K.A., Cowan, J.H., Winemiller, K.O., Myers, R.A., Hilborn, R., 2001. Compensatory density dependence in fish populations: importance, controversy, understanding and prognosis. Fish Fish. 2, 293–327.

Rosenberg, A.A., Swasey, J.H., Bowman, M., 2006. Rebuilding US fisheries: progress and problems. Front. Ecol. Environ. 4, 303–308.

Rothschild, B.J., 1998. Year class strengths of zooplankton in the North Sea and their relation to cod and herring abundance. J. Plankton Res. 20, 1721–1741.

Rothschild, B.J., Jiao, Y., Hyun, S.-Y., 2012. Simulation study of biological reference points for summer flounder. Trans. Am. Fish. Soc. 141, 426–436, http://dx.doi.org/10.1080/00028487.2012.667041

Safina, C., Rosenberg, A.A., Myers, R.A., Quinn II, T.J., Collie, J.S., 2005. U.S. ocean fish recovery: staying the course. Science 309, 707–708.

Scharf, F.S., Juanes, F., Rountree, R.A., 2000. Predator size–prey size relationships of marine fish predators: interspecific variation and effects of ontogeny and body size on trophic-niche breadth. Mar. Ecol. Ser. 208, 229–248.

Sissenwine, M.P., 1984. Why do fish populations vary? In: May, R.M. (Ed.), Exploitation of Marine Communities. Springer-Verlag, Berlin, pp. 59–94.

Solomon, M.E., 1949. The natural control of animal populations. J. Anim. Ecol. 18, 1–35, http://dx.doi.org/10.2307/1578

Staudinger, M.D., 2006. Seasonal and size-based predation on two species of squid by four fish predators on the Northwest Atlantic continental shelf. Fish. Bull. 104, 605–615.

Stevens, M., Maes, J., Ollevier, F., 2006. A bioenergetics model for juvenile flounder *Platichthys flesus*. J. Appl. Ichthyol. 22, 79–84.

Terceiro, M., 2002. The summer flounder chronicles: science, politics, and litigation, 1975–2000. Rev. Fish Biol. Fish. 11, 125–168.

Terceiro, M., 2011. Stock Assessment of Summer Flounder for 2011. National Oceanic and Atmospheric Administration, National Marine Fisheries Service.

Verheye, H.M., 2000. Decadal-scale trends across several marine trophic levels in the Southern Benguela upwelling system off South Africa. AMBIO 29, 30, http://dx.doi.org/10.1639/0044-7447-29.1.30

Ware, D.M., Thomson, R.E., 2005. Bottom-up ecosystem trophic dynamics determine fish production in the Northeast Pacific. Science 308, 1280–1284, http://dx.doi.org/10.1126/science.1109049.